

Low-Temperature Short-Time SPS Processes to Produce Fine-Grained High-Coercivity Barium Hexaferrite Ceramics from Polyol Nanoparticles

G. Vázquez-Victorio^{1,2} · N. Flores-Martínez² · G. Franceschin²  · S. Nowak² · S. Ammar²  · R. Valenzuela^{1,2} 

Received: 14 June 2017 / Accepted: 20 June 2017 / Published online: 30 June 2017
© Springer Science+Business Media, LLC 2017

Abstract Barium hexaferrite ($\text{BaFe}_{12}\text{O}_{19}$) ceramics were obtained by combination of polyol-synthesized precursors subsequently consolidated by spark plasma sintering (SPS) at a low temperature (800 °C). X-ray powder diffraction studies showed the influence of the experimental parameters to produce a virtually single- or multiphase material. The room temperature magnetic properties exhibited interesting variety of properties, including exchange coupling (spring magnet) between hexaferrite and other magnetic phases. The saturation magnetization and coercive field, at room temperature, are in the 34–70 emu/g and 4.1–5.0 kOe ranges, respectively. The combination of strong coercive field and magnetization resulted in a maximum energy product $[(\text{BH})_{\text{max}}] = 10.9 \text{ kJ/m}^3$ for the sample with the highest $\text{BaFe}_{12}\text{O}_{19}$ content.

Keywords Barium hexaferrite · Reactive spark plasma sintering · Nanostructures · Permanent magnet

1 Introduction

In spite of impressive progress in rare earth permanent magnet (PM) technology, bulk hexaferrites $\text{M}^{2+}\text{Fe}_{12}\text{O}_{19}$ (M^{2+} is a divalent cation, typically Ba, Sr) retain a dominant fraction

of the world permanent magnets' market, due to their inexpensive primary sources and a well-known “mature” technology [1]. Many efforts in the research activity are currently oriented to the enhancement of magnetic properties of these materials mainly by cation substitutions [2, 3] and reduction to the nanometric size range [4–6]. Another aspect with intense research activity is the investigations on preparation technology by means of inexpensive methods at lower sintering temperatures [7]. Recent developments on soft chemistry and sintering are leading to more performing nanostructured hexaferrites, through an appropriate control of microstructure.

In this work, we show that a combination of polyol-synthesized precursors subsequently consolidated by reactive spark plasma sintering (RSPS) can lead to materials with a very high energy product, and hence, a large variety of PM applications. The experimental parameters can be tailored to produce a virtually pure hexagonal, free from other iron oxide phases. A detailed analysis of the magnetic properties of obtained materials shows additionally that multiphase materials can provide an interesting variety of properties, including exchange coupling between magnetic phases [8]. Such materials can be useful in many applications. Here, we report results obtained from selected samples; the complete study involves a much larger investigation, which will be published later.

2 Experimental

2.1 Preparation of M-type Barium Hexaferrite Nanoparticles by Polyol Process (Precursors)

According to the classical procedure [9, 10], barium hydroxide, $\text{Ba}(\text{OH})_2 \cdot 8\text{H}_2\text{O}$, and iron nitrate, $\text{Fe}(\text{NO}_3)_3 \cdot 9\text{H}_2\text{O}$,

✉ G. Vázquez-Victorio
gvazquezvic@gmail.com

¹ Instituto de Investigaciones en Materiales, Universidad Nacional Autónoma de México, Ciudad de México 04510, México

² Laboratoire ITODYS, Sorbonne Paris Cité, CNRS-UMR, Université de Paris-Diderot, 7086, Paris, 75205, France

were dissolved in the stoichiometric ratio in a polyol. In this work, we used diethylene glycol (DEG) for some samples, and tetraethylene glycol (TTEG) for others as described in Table 1. We also tested the effects of the hydrolysis ratio h , which is defined as the water-to-metal molar total ratio. Taking into account that the water provided by the reagents led to $h = 9$; in some cases, extra water was added to reach $h = 15$, as described also in Table 1. The solution was carried out under argon atmosphere and mechanical stirring for 4 h. The mixture was heated up to its boiling point at a 6 °C/min heating rate under mechanical stirring, and maintained in reflux for 3 h more. The resulting suspension was then allowed to cool down to room temperature and the precipitated solid was recuperated by centrifugation, washed three times with ethanol, and was then left drying overnight at 60 °C. All powders were annealed in air at 800 °C for 1 h and subsequently used as starting materials to produce nanostructured barium ferrite ceramics by RSPS process.

2.2 BaFe₁₂O₁₉ Consolidation by RSPS

The consolidation of all powders was performed under vacuum using an SPS apparatus, model Dr. Sinter 511S Syntex. In order to test the effects of RSPS parameters, two main protocols were used: a high-pressure low-temperature one, by sintering at 290 °C for 8 min at 600 MPa (sample D5), and the opposite, i.e., high temperature (800 °C for 5 min) at a relatively low pressure, 100 MPa (samples T10 and T8). The pellets were then polished to remove any traces of carbon paper (“papiex”) used during the consolidation process.

2.3 Characterization

Structural characterization were performed by x-ray diffraction (XRD) using a Panalytical XpertPro equipped with a multichannel detector (X'celerator) using Co-K α radiation ($\lambda = 1.7889$ Å) in the 15°–100° 2θ range and a scan step of 0.25 for 2 s. A quantitative phase analysis was carried out using Rietveld refinements with the MAUD software. Information about the particles size and morphology were obtained from scanning electron microscopy (SEM) investigations using a JEOL-JSM 6100 microscope. Magnetic

hysteresis loops for RSPS-consolidated pellets were measured at room temperature in a maximum applied field of 7 Tesla using a Quantum Design MPMS[®]3 SQUID magnetometer in VSM mode.

3 Results and Discussion

3.1 Polyol Synthesis

After annealing at 800 °C, the XRD patterns of powders revealed the presence of the desired BaFe₁₂O₁₉ phase (JCPDS 98-006-0984), with variable amounts of other phases, α -Fe₂O₃ (JCPDS 98-008-2134) and BaFe₂O₄ (JCPDS 98-000-2769), as shown in Fig. 1. The results of the XRD analysis as a function of synthesis parameters have been gathered in Table 1.

D5 sample was synthesized with DEG and $h = 15$; it showed some ferrite (BaFe₂O₄), a low content of hexaferrite, and a large amount of hematite. DEG was changed by TTEG and to reduce the hematite content, we tested an h value of 9 (no water added in addition to water provided by the reagents) to obtain sample T10; the amount of hexaferrite increased. As TTEG seemed to favor the hexaferrite content, we increased again the h value to 15, resulting in an even larger content of the desired hexaferrite phase, sample T8. These samples were then sintered by RSPS, as explained below.

3.2 Sintered Ceramics

The relevant parameters and results from RSPS can be found in Table 2. We first carried out RSPS at very low temperature (290 °C, for 8 min) and very high pressure

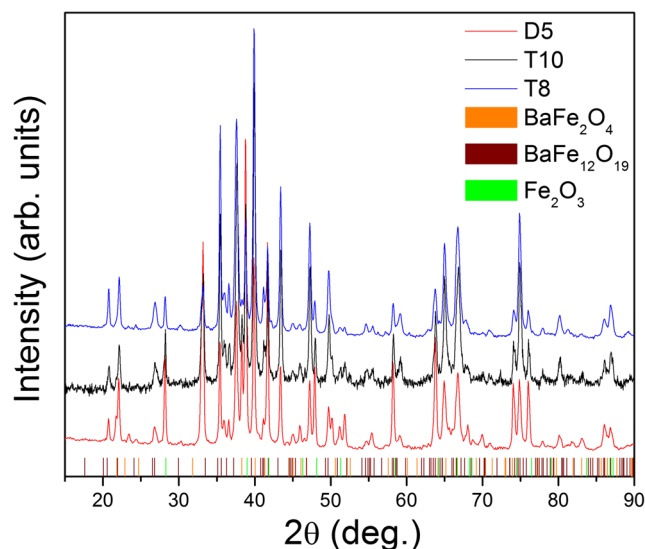


Fig. 1 XRD patterns of annealing powders before SPS process

Table 1 Synthesis parameters of polyol method and composition of RSPS precursor (powders) after annealing at 800 °C

Sample	Polyol	Hydrolysis ratio (h)	BaFe ₁₂ O ₁₉ (wt%)	α -Fe ₂ O ₃ (wt%)	BaFe ₂ O ₄ (wt%)
D5	DEG	15	25	65	10
T10	TTEG	9	68	24	8
T8	TTEG	15	79	18	3

Table 2 RSPS parameters, composition, and density of final pellets

Sample	Temperature (°C)	Time (min)	Pressure (MPa)	BaFe ₁₂ O ₁₉ (wt%)	α-Fe ₂ O ₃ (wt%)	BaFe ₂ O ₄ (wt%)	Fe ₃ O ₄ (wt%)	Density (g/cm ³)
D5	290	8	600	43	50	7	0	5.56
T10	800	5	100	40	0	10	50	5.18
T8	800	5	100	99	1	0	0	5.09

(600 MPa) for D5 sample. This low temperature was selected in order to avoid the grain growth, and a high pressure was proposed to reach a dense material. Refined XRD patterns (Fig. 2) showed an increase in hexaferrite phase (43 wt%) in spite of the low sintering *T*. Hexaferrite was accompanied by hematite and a small amount of Ba ferrite.

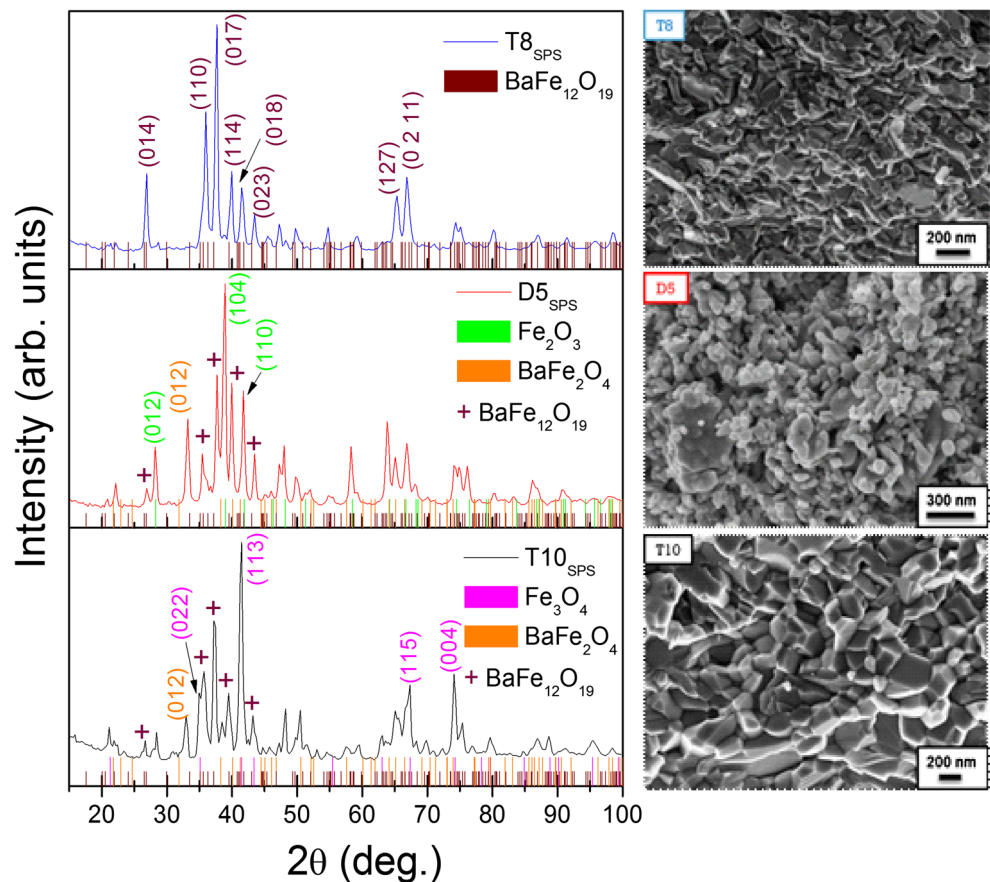
We then sintered the NPs synthesized with a reduced hydrolysis ratio (*h* = 9), which is labeled as T10. RSPS was carried out at a high temperature (800 °C, for 5 min) and low pressure (100 MPa). The XRD analysis revealed the absence of hematite, but a considerable amount of its reduced phase, magnetite (JCPDS 98-015-9976) was found, see Table 2. The formation of magnetite during the consolidation by the SPS process has been previously reported [11] and attributed to the strong reducing character of SPS [12]. Additional to magnetite, T10 sample contained about

10 wt% of BaFe₂O₄. Therefore, a decrease in the hydrolysis ratio did not favored the formation of hexaferrite.

We then decided to carry out RSPS in the same conditions (800 °C, for 5 min and low pressure, 100 MPa), for the T8 sample, which possessed a high hydrolysis ratio (*h* = 15). This time, XRD pattern showed a single phase (99 wt%, with just traces of Ba ferrite) with all diffraction peaks assigned to BaFe₁₂O₁₉ phase, as appears in Fig. 2.

The morphological information about samples was obtained from the SEM micrographs, shown in Fig. 2. D5 sample revealed irregular grain shapes with a small size as expected for this sample sintered at very low temperature. Micrographs from T10 and T8 samples showed a faceted material with larger grain size, in agreement with the increase in sintering temperature, and there is clear evidence that some grains have coalesced to form larger grains due to the high temperature. In all cases, the samples exhibited,

Fig. 2 XRD patterns and SEM images of final pellets



however, an average grain size below 500 nm, lower than the values found in literature for sintered BaFe₁₂O₁₉ samples with classic methods [13]. This is a direct consequence of the short sintering time and low temperature involved in RSPS [14].

Figure 3 shows the magnetic hysteresis loop for T8 sample. Saturation magnetization ($M_s = 70$ emu/g) and coercive field ($H_c = 4.1$ kOe) are in good agreement with the bulk values reported for barium hexaferrite (BaFe₁₂O₁₉) [1]. The combination of strong coercive field and magnetization and the tendency to a square loop resulted in the largest energy value found in this work, $(BH)_{max} = 10.9$ kJ/m³. This is larger than the typical reported values for polycrystalline, not-oriented samples [11]. With the pertinent preparation parameters, RSPS can therefore produce a single-phase, dense, nanostructured material with improved magnetic properties. For comparison, the magnetic parameters of all samples have been gathered in Table 3.

The analysis of the magnetic properties of other samples is quite meaningful. The D5 sample values of M_s and H_c are 34 emu/g and 5 kOe, respectively. A decrease in magnetization value (both saturation and remanent) is observed, due to the presence of the antiferromagnetic (AF) phase (hematite). This dilution effect, in addition to the small grain size obtained by the low sintering temperature used, exhibited the highest H_c value reported in this investigation. This result can be understood in terms of the isolation of small, single-domain hexaferrite grains surrounded by AF hematite grains, which break the tendency to continuity in magnetic flux between ferrimagnetic grains. A similar effect has been observed in cobalt ferrite mixed with a non-magnetic phase [15]. The $(BH)_{max}$ value decreased to 2.1 kJ/m³ due to the decrease in M_r value and a reduction of the square shape in the hysteresis loop, see Fig. 3.

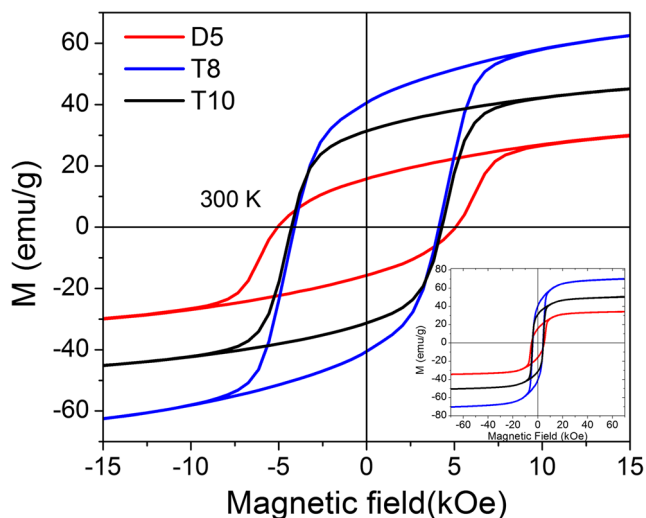


Fig. 3 Hysteresis loops of consolidated ceramics at room temperature

Table 3 Magnetic properties at room temperature of consolidated samples

Sample	H_c (kOe)	M_s at 7 T (emu/g)	M_r (emu/g)	$(BH)_{max}$ (kJ/m ³)
D5	5	34	16	2.1
T10	4.3	50	31	7.4
T8	4.1	70	41	10.9

Last but not least, T10 sample presents $M_s = 50$ emu/g and $H_c = 4.3$ kOe. In spite of the low content of barium hexaferrite, M_s value increases due to the amount of magnetite ($M_s = 90$ emu/g [16]) formed during the RSPS process. Magnetite was formed because of a low hydrolysis ratio and the RSPS reducing conditions. RSPS is indeed a reductive process, as recently shown in the case of Ni–Zn ferrite sintering [12]. Magnetite is a soft material with a higher magnetization value and during measurements, it is the total value of magnetization (contribution of all magnetic moments in the volume) which is detected. However, what is remarkable is that in spite of the low value of H_c of magnetite (typically below 200 Oe), the coercive field value of this sample is high, comparable to sample T8 (virtually pure hexaferrite phase). The absence of a “shoulder” in the hysteresis loop (at the expected value of the coercive field of magnetite) and the presence of a single H_c , as shown in Fig. 3, can be explained by an exchange coupling between the two ferrimagnetic phases. The soft phase is “driven” by the hard phase and the material behaves as a single magnetic entity. This phenomenon is known as *spring magnet* and allows to maintain a high H_c value while increasing the magnetization value [8]. The $(BH)_{max}$ is 7.4 kJ/m³, a high value for a sample with such low content of hard magnetic material.

4 Conclusions

By means of a good choice of preparation parameters, the combination of polyol-synthesized NPs, subsequently consolidated by reactive spark plasma sintering (RSPS) can lead to single-phase nanostructured barium hexaferrite with enhanced magnetic properties. These parameters included, for the polyol synthesis, the use of tetraethylene glycol and a hydrolysis ratio of 15. For the RSPS sintering, the optimal conditions were 800 °C at a pressure of 100 MPa for 5 min. As expected, the single-phase hexaferrite obtained exhibited a high energy product $(BH)_{max}$. Variations in these parameters resulted in other phases present in the final material, in addition to the hexagonal ferrite. A careful analysis of such materials showed unusual magnetic properties; a very high coercive field as a consequence of the dilution

of small hexaferrite grains, as well as evidence of exchange coupling (also known as spring magnets) associated with the presence of a soft ferrimagnetic phase (magnetite). The synthesis and sintering parameters involved in this proposed process therefore allow the tailoring of magnetic properties, and can provide novel materials for specific applications.

References

- Pullar, R.C.: Hexagonal ferrites: a review of the synthesis, properties and applications of hexaferrite ceramics. *Prog. Mater. Sci.* **57**(7), 1191–1334 (2012). doi:[10.1016/j.pmatsci.2012.04.001](https://doi.org/10.1016/j.pmatsci.2012.04.001)
- Haq, A., Anis-ur-Rehman, M.: Effect of Pb on structural and magnetic properties of Ba-hexaferrite. *Physica B* **407**, 822–826 (2012). doi:[10.1016/j.physb.2011.11.038](https://doi.org/10.1016/j.physb.2011.11.038)
- Ghzaïel, T.B., Dhaoui, W., Pasko, A., Mazaleyrat, F.: Effect of non-magnetic and magnetic trivalent ion substitutions on BaM-ferrite properties synthesized by hydrothermal method. *J. Alloys Compd.* **671**, 245–253 (2016). doi:[10.1016/j.jallcom.2016.02.071](https://doi.org/10.1016/j.jallcom.2016.02.071)
- González-Carreño, T., Morales, M.P., Serna, C.J.: Barium ferrite nanoparticles prepared directly by aerosol pyrolysis. *Mater. Lett.* **43**(3), 97–101 (2000). doi:[10.1016/S0167-577X\(99\)00238-4](https://doi.org/10.1016/S0167-577X(99)00238-4)
- Xu, P., Han, X., Wang, M.: Synthesis and magnetic properties of BaFe₁₂O₁₉ hexaferrite nanoparticles by a reverse microemulsion technique. *J. Phys. Chem. C* **111**(16), 5866–5870 (2007)
- Drofenik, M., Ban, I., Makovec, D., Žnidaršič, A., Jagličić, Z., Hanžel, D., Lisjak, D.: The hydrothermal synthesis of superparamagnetic barium hexaferrite particles. *Mater. Chem. Phys.* **127**, 415–419 (2011). doi:[10.1016/j.matchemphys.2011.02.037](https://doi.org/10.1016/j.matchemphys.2011.02.037)
- Orrù, R., Licheri, R., Locci, A.M., Cincotti, A., Cao, G.: Consolidation/synthesis of materials by electric current activated/assisted sintering. *Mater. Sci. Eng., R* **63**(4), 127–287 (2009). doi:[10.1016/j.mser.2008.09.003](https://doi.org/10.1016/j.mser.2008.09.003)
- Kneller, E.F., Hawig, R.: The exchange-spring magnet: a new principle for permanent magnets. *IEEE Trans. Mag.* **27**(4), 3588–3600 (1991). doi:[10.1109/20.102931](https://doi.org/10.1109/20.102931)
- Beji, Z., Smiri, L.S., Yaacoub, N., Greneche, J.M., Menguy, N., Ammar, S., Fievet, F.: Annealing effect on the magnetic properties of polyol-made Ni-Zn ferrite nanoparticles. *Chem. Mater.* **22**(4), 1350–1366 (2010). doi:[10.1021/cm901969c](https://doi.org/10.1021/cm901969c)
- Gaudisson, T., Acevedo, U., Nowak, S., Yaacoub, N., Greneche, J.M., Ammar, S., Valenzuela, R.: Combining soft chemistry and spark plasma sintering to produce highly dense and finely grained soft ferrimagnetic Y₃Fe₅O₁₂ (YIG) ceramics. *J. Am. Ceram. Soc.* **96**(10), 3094–3099 (2013). doi:[10.1111/jace.12452](https://doi.org/10.1111/jace.12452)
- Stingaciu, M., et al.: Magnetic properties of ball-milled SrFe₁₂O₁₉ particles consolidated by Spark-Plasma Sintering. *Sci. Rep.* **5**, 14112 (2015). doi:[10.1038/srep14112](https://doi.org/10.1038/srep14112)
- Valenzuela, R., Gaudisson, T., Ammar, S.: Severe reduction of Ni-Zn ferrites during consolidation by spark plasma sintering (SPS). *J. Magn. Magn. Mater.* **400**, 311–314 (2016). doi:[10.1016/j.jmmm.2015.07.044](https://doi.org/10.1016/j.jmmm.2015.07.044)
- Shepherd, P., Mallick, K.K., Green, R.J.: Magnetic and structural properties of M-type barium hexaferrite prepared by coprecipitation. *J. Magn. Magn. Mater.* **311**(2), 683–692 (2007). doi:[10.1016/j.jmmm.2006.08.046](https://doi.org/10.1016/j.jmmm.2006.08.046)
- Franceschin, G., Flores-Martínez, N., Vázquez-Victorio, G., Ammar, S., Valenzuela, R.: Sintering and reactive sintering by spark plasma sintering (SPS). In: Shishkovsky, I.V. (ed.) *Sintering*. Intechopen (In Press)
- Acevedo, U., Gaudisson, T., Ortega-Zempoalteca, R., Nowak, S., Ammar, S., Valenzuela, R.: Magnetic properties of ferrite-titanate nanostructured composites synthesized by the polyol method and consolidated by spark plasma sintering. *J. Appl. Phys.* **113**, 17B519 (2013). doi:[10.1063/1.4798604](https://doi.org/10.1063/1.4798604)
- Valenzuela, R.: *Magnetic Ceramics*, p. 129. Cambridge University Press, Cambridge (2005)